

Synthesis, Characterization and Alignment of Mn²⁺ and/or Eu³⁺ Doped Cadmium Telluride Nanowires

Volkan Cicek*, Mehmet Ozdemir**

*(Faculty of Science and Engineering, Ishik University, Erbil, Iraq)

** (Faculty of Education, Ishik University, Erbil, Iraq)

Abstract

The foremost objective of the proposed research is to synthesize magnetically-active CdTe nanowires that can be manipulated by magnetic fields. The ability to do so will facilitate fabrication of molecular electronics and a whole host of other potential applications. The research will employ doping of CdTe with either Mn²⁺ or Eu³⁺ or a mixture of both to create nanoparticles with net magnetic moments. The particles size and morphology will be probed by AFM and TEM while the extent of doping and distribution of dopant ions will be determined by bulk analysis by ICP, surface analysis by XPS, EPR and X-ray powder diffraction. The magnetic moment and magnetic ordering will be determined by use of a SQUID magnetometer. Doped CdTe particles with suitable magnetic moments will then be converted to CdTe wires using a technique originally developed for undoped CdTe. The changes in morphology, size, composition, and structure will be monitored using the same analytical methods used for characterization of the precursor nanoparticles. Finally, nanowires that possess a sufficient magnetic moment will be aligned using a magnetic field to prove the viability of this approach for manufacturing nanoscale devices and electronics.

Key words: dopant, morphology, nanowire, lithography, paramagnetism

1. Introduction

Nanostructures (that is, structures with at least one dimension between 1 and 100 nm) have attracted steadily growing interest due to their fascinating properties, as well as their unique applications relative to their bulk counterparts. Nanowires, by definition, are anisotropic nanocrystals with large aspect ratios (length/diameter). Generally, they would have diameters of 1-200 nm and length up to several tens of micrometers. Nanowires differ significantly from spherical nanocrystals by their morphology as well as physical and electronic properties. The ability to generate such structures is now central to the advance of many areas in modern science and technology.

Over the past few decades there has been tremendous growth in the computer and communications industries. In part, this growth has been spurred by the continual miniaturization of electronic components. As predicted by Moore in 1965, the density of transistors on a Si chip has doubled every 18 months¹. However, in order to maintain this growth, a great deal of capital has been invested in lithographic methods. Even though lithography techniques presently enjoy a complete domination of the electronics industry, they grow exponentially more expensive with decreasing feature size, and may never reach the dimensions required for this new technology. Due to these limitations, it has been suggested that future device integration may be based on alternative approaches that rely on assembly of nanometer-scale colloidal particles. One approach that is showing a lot of promise is molecular electronics, a method that uses molecules to act as wires, diodes, and resistors. Rather than the "top-down" approach of lithography, molecular electronics allows devices to be designed and built on the atomic scale, from the "bottom-up." Therefore, research has focused on developing new chemical, magnetic, and electric field assisted assembly techniques to control the placement of these particles with the precision required to form well-ordered logic and memory circuits. Although there have been several successes with this method, there is still a lack in the middle scale of 10-200 nm. Technology is required that can connect molecular scale devices to the macroscale world and it is proposed that nanowires can be used in this role.¹

On the other hand, the use of both the spin and the charge of electrons in semiconductors have long been sought for the storage and processing of information for electronic devices. Since 1990 the magnetic storage density of hard disk drives increased about 60% per year.

- Commercial (1980s): 1Mbit/in² (1 Bit = 25 m x 25 m)
- Commercial (1997): 1 Gbit/in² (1 Bit = 800 nm x 800 nm)
- Commercial (2000): 10 Gbit/in² (1 Bit = 250 nm x 250 nm)
- Commercial (2002): 50 Gbit/in² (1 Bit = 110 nm x 110 nm)

- What comes after 50 Gbit/in²? Fundamental limits (100 nm) will be reached.
- Search for a new storage paradigm: maybe single domain storage (quantum magnetic disc)

The limits of magnetic storage: Super paramagnetic limit

- Today's magnetic storage media are unstructured.
- Signal-to-noise considerations demand >1000 polycrystalline grains per bit
- Increasing the storage density with constant signal-to-noise ratio demands reducing size of grains not number of grains.
- As grain size decreases, energy to switch magnetization decreases
- When the energy needed to switch magnetization becomes smaller than thermal energy, thermal fluctuations will flip the magnetization of grains and the storage medium becomes unstable. This is called super paramagnetism

Storing each bit in a single magnetic domain (magnetic nanostructure) pushes the super paramagnetic limit to approx. 100 times higher storage density.²

Magnetic nanowires could be the solution for the aforementioned two problems, which are connecting molecular scale devices to the macroscale world and pushing the super paramagnetic limit to approximately 100 times higher storage density. Therefore, successful synthesis and alignment of magnetic nanowires is of great importance which is why as it is chosen as the objective of this proposed research.

Semi-magnetic or diluted magnetic semiconductor nanoparticles are the most promising precursors for the synthesis of magnetic nanowires. Diluted magnetic semiconductors are alloys in which a magnetic ion (Mn²⁺, Fe²⁺, Co²⁺) is diluted in the structure of a nonmagnetic A^{II}B^{VI} semiconductor host (CdS, CdTe, ZnSe., etc.). The presence of localized magnetic ions in a semiconductor alloy modifies the optical properties and leads to different types of magnetic behavior.³ Therefore, these semi-magnetic semiconductors exhibit a number of interesting magneto-optical effects such as giant Faraday rotation, large Zeeman splitting of carriers, and bound magnetic polarons.

The addition of impurity elements to a host lattice is a common approach for tuning electronic, optical, mechanical, and magnetic properties of materials. However, in the case of nanostructured materials, their small size and large surface area-to-volume ratios present a significant challenge to impurity doping. Extremely high doping concentrations must be achieved to incorporate a

meaningful number of atoms into the structure. For example, 12 Mn impurity atoms in a 4 nm diameter InAs semiconductor nanocrystal correspond to a doping concentration greater than 10²⁰ cm⁻³ (compare this to typical n- and p- dopant levels in silicon of 10¹⁶ to 10¹⁸ cm⁻³!).⁴ Doping levels of this magnitude often exceed the solubility limits of the impurity element in the host lattice. Furthermore, high dopant solubility does not guarantee effective nanostructure doping. Accordingly, the term doping should be considered as describing other locations of the foreign ions such as binding to the surface capping ligands or adsorption on the nanocrystal surfaces.

Architectural control of the anisotropic nanocrystals including one-dimensional wires and the reliable incorporation of desired dopants are imperative for the success of bottom-up nanodevice applications, not to mention the novel scientific features that accompany them. In a previous study, TEM and EDAX (Energy dispersive X-ray) analyses demonstrated that Cd_{1-x}Mn_xS nanorods could be prepared that were ~7nm in width with an aspect ratio of ~4 at maximum doping levels up to ~12%.⁵ Except in some cases, the formation of diluted magnetic semiconductor nanocrystals with a homogeneous distribution at high level of Mn doping has been difficult because of facile segregation of Mn dopants from the host matrix. Therefore, to confirm homogenous distribution of Mn atoms inside the CdS matrix, ligand exchange experiments with pyridine were first performed, which removes Mn atoms bound to the surfaces of host nanocrystals. In the case of Mn atoms residing on the surfaces of host matrix, a huge decrease of Mn composition is expected. However, in the study of Cd_{1-x}Mn_xS rods, even after three times repetition of ligand exchange processes, only slight decreases of Mn composition appeared in EDAX. This result indicates Mn atoms are not heavily localized on the surfaces of nanocrystals. Embedding of Mn inside the matrix is also inferred from EPR (Electron paramagnetic resonance) measurements. Because hyperfine splitting constants depend on the environments of Mn atoms, the bonding characteristics between Mn atoms and host lattices can be explained by EPR analysis. In the case of low concentrations of Mn (~2%), six hyperfine splittings due to Mn (I=5/2) were clearly observed that is attributed to Mn-Mn interactions. The observed splitting constant is consistent with the occupation of Mn on tetrahedral sites of the internal CdS matrix. Mild growth conditions are needed for high-level doping of Mn. For example, at high temperature (~300 °C) with otherwise identical procedures, only poorly doped Cd_{1-x}Mn_xS nanorods (x < 0.02) were obtained, where most of the Mn atoms seem to be annealed out of CdS lattices under supply of sufficient thermal energy.

Many publications show that exchange interactions, which couple Mn spins antiferromagnetically, play a dominant role in the magnetic studies of diluted magnetic semiconductor materials.³ S_{eff} is the effective mean spin of the Mn^{2+} ions and is always smaller than 5/2. This is due to antiferromagnetic Mn^{2+} - Mn^{2+} interactions that reduce the formation of spin pairs with a zero total magnetization. The magnetic moment decreases with increasing Mn^{2+} composition since the probability of magnetic ions occupying neighboring sites increases. Considering antiferromagnetic coupling, one can come up with following theoretical discussion.

i) The S_{eff} values of nanocrystals are smaller than those determined in the bulk phase. This indicates that the number of spins correlated in antiferromagnetic clusters is higher in nanoparticles. This means that the Mn^{2+} - Mn^{2+} interactions in $\text{Cd}_{1-x}\text{Mn}_y\text{S}$, $\text{Cd}_{1-x}\text{Mn}_y\text{Se}$, $\text{Cd}_{1-x}\text{Mn}_y\text{Te}$ nanocrystals are larger than those in the bulk phase.

ii) At a fixed composition of the dopant, the S_{eff} value decreases with decreasing particle size. Thus, interactions between spins increase with decreasing particle size.

iii) For a given particle size, the S_{eff} value decreases with increasing composition of the dopant. The fraction of Mn^{2+} ions that forms pairs with antiferromagnetic interaction understandably increases with the amount of manganese in the nanocrystals.

iv) The S_{eff} values decrease with decreasing temperature. This is due to the decrease of thermal motion with temperature that allows the spins to interact more easily with their neighbors. These data indicate an increase in the Mn^{2+} - Mn^{2+} interactions (S_{eff}) with decreasing the particle size.

However, in contrast to the theoretical expectations, recent experiments on Mn-doped ZnS nanocrystals showed unusual magnetization properties. In bulk ZnS:Mn, Mn ions are ferromagnetically coupled via the exchange interaction, thereby M at low temperatures is significantly reduced, which suggests the presence of strong antiferromagnetic interactions. On the other hand, there is no antiferromagnetic interaction between Mn atoms within ZnS:Mn nanocrystals, which suggests that the Mn ion exists as a single impurity, and Mn-Mn pairs are not likely to exist inside the nanocrystal. This is consistent with the Mn concentration, which was 0.28 mol%, which is same as that of the ZnS:Mn nanocrystal with one Mn ion per nanocrystal with the diameter of 3 nm. The limit of one Mn ion per nanocrystal has also been suggested for ZnSe:Mn and CdS:Mn. Other measurements revealed that there are 4 Mn ions on average per nanocrystal. However, most of these Mn ions are coordinated on the surface, and since antiferromagnetic interactions are not present, these Mn ions on the surface do not interact magnetically. It is supposed that the d orbitals of the Mn ions on

the surface are only weakly hybridized with the host wave function.⁶

In another study on Mn-doped ZnS nanocrystals, it was reported that the dopant atoms were distributed inhomogeneously within the antiferromagnetically doped nanocrystals. This simple inhomogeneous doping model suggests that interior dopant atoms are localized within the crystal.⁷ One coherent example is Mn doped ZnO nanocrystals. The electron paramagnetic resonance spectra from the doped samples, that is similar to the bulk Mn-doped ZnO, exhibit well-resolved hyperfine splitting, which is a characteristic of isolated Mn^{2+} ions. This suggests that the Mn-Mn interactions are rather weak establishing that the Mn^{2+} ions are randomly distributed in the ZnO matrix without any significant clustering. The value of the coupling constant suggests that Mn^{2+} is in a tetrahedral environment, rather than in the usually preferred octahedral environment of Mn^{2+} ions. As a result, XRD patterns suggest the formation of wurtzite nanocrystals with a size of 4.7 nm in such cases. EPR and XAS measurements establish the presence of Mn^{2+} substitutionally incorporated in the interior as well as in the surface region of the nanocrystals.⁸

It is also observed that reaction-limited aggregation of paramagnetic Co^{2+} : ZnO at room temperature gives rise to robust ferromagnetic ordering with $T_c > 350$ K. The metastable band gap energy of Co^{2+} : ZnO increases linearly as the initial Co^{2+} concentration increases, and the band gap intensity is inversely proportional to the Co^{2+} concentration. Similarly, the Ni^{2+} : ZnO band gap energy increases with introduction of Ni^{2+} , but further increases in initial Ni^{2+} mole percent above 1% have little effect on the ZnO band gap energy. The trend observed for the dependence of the band gap intensity on initial Ni^{2+} concentration is similar to that observed for Co^{2+} doping. The $S = 3/2$ saturation magnetization behavior of ZnO band gap MCD (Magnetic circular dichroism) intensity indicates magnetization of the semiconductor due to interaction with the Co^{2+} dopants, where MCD is an optical probe of paramagnetism that details the electronic and magnetic properties of the ground states of metal centers. This phenomenon, the so-called "giant Zeeman effect", is of central importance to the potential spin-electronics applications of this diluted magnetic semiconductor material. The exchange interaction between the dopant and a conduction band electron is coulombic and the covalency of the oxo- Co^{2+} bond gives rise to strong direct antiferromagnetic exchange between the dopant and an unpaired valence band electron.⁹

In the case of ZnS:Eu nanocrystals, since $\text{Eu}(\text{NO}_3)_3$ is used as a dopant, Eu ions are expected to incorporate as Eu^{3+} . However, χ (T) and M of ZnS:Eu nanocrystals show a distinct contrast to those of Eu^{3+} ions of $\text{Eu}(\text{NO}_3)_3 \cdot 6\text{H}_2\text{O}$ powder. This

fact suggests that a substantial amount of Eu ions are reduced to magnetic Eu^{2+} . Between 200 and 300 K, Eu^{2+} and Eu^{3+} coexist with the concentrations of 0.035 and 0.018 mol%, respectively. Theoretically, the concentration of Eu^{2+} should give a saturation M of 14 emu/ZnS mol. However, the saturation M is found as small as 6 emu/ZnS mol. It is unclear whether this discrepancy is due to a possible antiferromagnetic interaction between Eu ions or not.⁶

Room temperature ferromagnetism has been reported for Co^{2+} , Fe^{2+} , and V^{2+} doped ZnO, but several other studies also report the absence of ferromagnetism in these materials.⁹

Although many studies have been reported on semiconductor materials doped with magnetic ions, there are many discrepancies in the data, that suggest the preparation method and the conditions significantly influence the properties of diluted magnetic semiconductor materials. Therefore, synthesis of nanoparticles doped with magnetic ions by using a fairly uncommon but successful technique is proposed. From these, nanowires of these magnetic ion doped nanoparticles will be synthesized by using another relatively less studied method. Furthermore, these synthesized nanowires will be magnetically aligned for use in molecular electronics.

2. Research Design and Methodology

2.1. Choice of Dopants

a) Mn^{2+}

Due to the host sp - Mn d interactions in diluted magnetic semiconductor materials, unusual magnetotransport and magneto-optical phenomena such as large Faraday rotations, giant negative magnetoresistances, and magnetic field induced metal-insulator transitions have been observed.¹⁴ It is reported that a single-impurity state for both ZnSe:Mn and CdS:Mn results in a giant internal field as high as 400 T on the conduction electrons of the nanocrystal. Further studies on the structure of these materials revealed that there is only single Mn^{2+} ions present for nanocrystal and the rest of the Mn^{2+} are coordinated on the surface and not incorporated into the nanocrystal core.⁶

For Mn-doped InAs, surface exchange and magnetic measurements confirmed that much of the dopant resides in the nanocrystal core and modifies the magnetic properties of the host material through antiferromagnetic superexchange interactions. The doping levels achieved are sufficiently high to expect ferromagnetism.¹⁷

In another study, doping Mn into the bulk ZnO matrix offers an interesting way to alter various properties, for example, the band gap of the host material can be tuned from 3.3 eV to 3.7 eV. It is also reported that Mn-doped ZnO thin films as well as in bulk exhibit ferromagnetism at room temperature.⁸

As suggested by many publications, Mn^{2+} ions lead to significant changes in both magnetic and optical properties of diluted magnetic semiconductor materials due to both their high magnetic moment of $S=5/2$ and relatively easier incorporation into the nanocrystal core of diluted magnetic semiconductor materials because of their size and charge. Consequently, since the purpose of this proposed research is to magnetically align CdTe nanowires for the construction of simple molecular circuits, Mn^{2+} ions are proposed as the primary dopant of CdTe nanocrystals.

b) Eu^{3+}

There are a number of papers reporting semiconductor nanocrystals doped with lanthanides ($\text{Ln}^{2+/3+}$) such as Tb^{3+} , Sm^{2+} or $\text{Eu}^{3+/2+}$; however, the successful incorporation of these ions into the inorganic core of the ZnS or CdS nanocrystals still needs to be demonstrated.^{8,11} One method of doping nanoparticles employs thiosalicylic acid. The thiol group of this acid binds to the nanocrystal surface while the carboxylic group is used as a complexing ligand for the lanthanide ions. Lanthanide ions are known as highly oxophilic, typical hard Lewis acids with little affinity for the sulfur ligands. Therefore, in water, only the carboxylic groups of the thiosalicylic acid are considered to bind the ion. Conversely, the Cd^{2+} ions are expected to bind both the sulfur and carboxyl moieties of the thiosalicylic acid molecule, with greater affinity for the thiol moiety.

Despite the absence of lifetime shortening, numerous papers on the luminescence of semiconductor nanoparticles doped with 3d transition metal ions or rare earth ions have appeared and in various articles it was concluded that both the transition metal and rare earth metal doped ZnS nanocrystals “form a new class of luminescent materials”. For Eu-doped ZnS nanocrystals, the magnetic susceptibility data reveal the coexistence of Eu^{2+} and Eu^{3+} ions, although the starting material contains only Eu^{3+} ions. It is notable that the Eu^{2+} state has no orbital moment L, which allows us to neglect the crystal field effect at low temperatures. Thus, we can assume that Eu^{2+} ions have full magnetic moment of $S=7/2$ down to 5 K.⁶

On the other hand, europium ions appear to form a solid solution with CdSe that has a random ion displacement of the cadmium cation site by the substitutional guest Eu^{3+} .¹¹

Nanocrystalline ZnS and CdS samples have been synthesized in the presence of Eu^{3+} and Tb^{3+} using various techniques (precipitation in water, methanol, or toluene and reverse micelle techniques) that have been reported to yield ZnS or CdS nanoparticles doped with luminescent rare earth ions. Since the ionic radius of the Cd ion is larger than the ionic radius of Zn^{2+} ion (0.98 and 0.74 Å,

respectively), it is expected that either Eu^{2+} or Eu^{3+} are incorporated more easily in CdS than in ZnS.¹²

The $\text{Eu}^{3+/2+}$ system has chosen as the second doping agent due to its potential to affect the magneto-optical properties of the diluted magnetic semiconductor materials.

c) Mn^{2+} and $\text{Eu}^{3+/2+}$

Co-doping can be particularly effective for frustrating anti-ferromagnetic ordering to yield a magnetic material. Theoretically, antiferromagnetic coupling interactions between two ions having different magnetic moments would yield a ferrimagnetic material rather than an antiferromagnetic material with a zero total magnetization. Therefore, co-doping of Mn^{2+} and $\text{Eu}^{3+/2+}$ system is also proposed along with the separate doping of Mn^{2+} and $\text{Eu}^{3+/2+}$ ions.

Additionally, co-doped semiconductors have promising features. For example, a novel luminescent property has been observed in the photoluminescence spectra of the ZnS nanoparticles co-doped with Ni^{2+} and Mn^{2+} .²⁶ Photoluminescent properties of the co-doped samples are found to be dramatically different from those of Ni^{2+} doped and Mn^{2+} doped ZnS nanoparticles. The ZnS nanoparticles can be doped with Ni^{2+} and Mn^{2+} during synthesis without altering the X-ray diffraction pattern.

2.2. Choice of Doping Technique

Previously, nanomaterials were synthesized by mixing the ionic reactants in a non-polar solvent at low temperatures. This procedure made it possible to form a very small amount of material. The control of particle growth is governed by several factors. The most commonly used one is electrostatic interactions between one of the reactants and an additive. For example, this process takes place when the chemical reaction is performed in the presence of a charged polymer in a colloidal solution. Another approach to prevent particle growth is to use a reactant that interacts selectively with the material formed. Organometallic compounds can be used as reactants where the particle size is controlled by varying the concentration and temperature. Other parameters can be used as mechanical constraints: sol-gel or glass matrices prevent diffusion of the reactants whereas with zeolites the pore size prevents the particle growth.¹³

The reverse micelle method is another commonly used method for the synthesis of nanocrystals, such as for synthesis of CdTe nanocrystals¹⁴, and for Mn^{2+} doping into CdS^3 . However; it does have some limitations.²³ As an example, while CdTe nanoparticles are synthesized successfully (2 to 4 nm in size)^{14,15}; $\text{Cd}_{1-y}\text{Mn}_y\text{Te}$, $\text{Zn}_{1-y}\text{Mn}_y\text{Te}$ or ZnTe structures that are thermodynamically stable in bulk phase could not be

fabricated in contrast to what was observed with $\text{Cd}_{1-y}\text{Mn}_y\text{S}$.¹³ In addition, the fact that nanocrystals are grown inside a droplet in this technique might not allow the nanoparticles to aggregate to form nanowires, which is the next step of this proposed study.

The chemical precipitation technique is also extensively used for synthesis of diluted magnetic semiconductor materials¹⁶. The synthesis technique proposed in this study for synthesis of doped-CdTe nanocrystals is also a chemical precipitation method. H. Weller, whose group first used and gradually improved the method since 1996, describes the advantages of CdTe nanocrystals synthesized by his method as high stability to oxidation, improved crystallinity, size- and surface-dependent absorption, and strong photoluminescence properties.

Although semiconductor nanocrystals such as CdS and CdSe can be successfully synthesized, nanocrystals of CdTe have proven difficult to synthesize by other methods. The high susceptibility of tellurium anions to oxidation is the main problem that is encountered. CdTe nanoparticles have been prepared through organometallic routes, by an exchange reaction between sodium telluride and cadmium iodide in methanol and by precipitation of Cd^{2+} ions in the presence of polyphosphate or both polyphosphate and thiols in aqueous solutions using NaHTe as the Te source. However, CdTe particles synthesized by these methods have not reached the nanocrystal quality of e.g. CdS and CdSe.¹⁶

Consequently, Weller's thiol-stabilized CdTe nanocrystal synthesis technique is chosen over other methods, because CdTe nanowires could be synthesized from the self-assembly of CdTe nanoparticles synthesized by this technique.¹⁷

3. Synthesis of Doped Nanoparticles and Doped Nanowires

3.1. Synthesis of Doped Nanoparticles

Magnetic ion doped CdTe nanoparticles will be synthesized according to Weller's method for pure CdTe with the introduction of a dopant during the reaction.

In the only similar study found in the literature, which is the synthesis of Mn-doped $\text{Cd}_{1-x}\text{Mn}_x\text{S}$ nanocrystals, followed by the synthesis of 1-D Mn-doped $\text{Cd}_{1-x}\text{Mn}_x\text{S}$ nanowires, a dopant solution of $\text{Mn}(\text{S}_2\text{CNET}_2)_2$ is introduced directly into CdS precursor solution of $\text{Cd}(\text{S}_2\text{CNET}_2)_2$ at 120 °C.⁵

Weller's method consists of three steps. First, H_2Te is generated by reaction of Al_2Te_3 with 0.5 M H_2SO_4 at 0°C under N_2 atmosphere. A 0.05 M NaHTe solution is then prepared by the titration of N_2 saturated 0.05 M NaOH with the prepared H_2Te at 0°C under N_2 atmosphere. After titration, the solution is bubbled with N_2 for 30 minutes to remove any traces of H_2Te present in the solution. Finally, in the presence of thioglycolic acid or

mercaptoacetic acid the solution of freshly prepared oxygen free NaHTe is added to a N₂ saturated solution of Cd(ClO₄)₂ in 125 ml H₂O, which had been previously adjusted to a pH of 11.2. The sizes of the particles will be controlled by the duration of

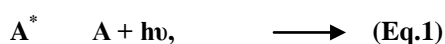
the heating process. In the proposed research the procedure will be modified by inclusion of Mn(ClO₄)₂ and/or Eu(ClO₄)₃ into the Cd(ClO₄)₂ solution in various amounts that are depicted in the following Table-1,

Table 1

Sample #	% Concentrations																
	1	2	3	4	5	6	7	8	9	10	11	12	13	14	15	16	17
Mn ²⁺	0.1	0.2	0.5	1.0	2.0	0	0	0	0	0	1.0	0.5	0.1	1.0	2.0	0.5	0.5
Eu ³⁺	0	0	0	0	0	0.1	0.2	0.5	1.0	2.0	1.0	0.5	0.1	0.5	0.5	1.0	2.0

Higher dopant concentrations may be tried, although segregation of dopant atoms out of the CdTe matrix is more likely to occur. As the first synthesizers of CdTe nanoparticles with the mentioned experimental method, Weller's group described the physical properties of CdTe nanoparticles by using different techniques.¹⁶ Powder X-ray diffractometry revealed that these nanoparticles have predominantly the cubic blende crystalline structure. This phase is also favorable for bulk CdTe. Notably, a predominant wurtzite crystalline structure has been observed for CdTe nanoparticles prepared by means of other methods. Fourier analysis of high-resolution micrographs of single CdTe particles also revealed a cubic structure of the nanocrystallites with 3% larger lattice constants compared to that of bulk CdTe. This discrepancy could be a consequence of the preparative conditions: whereas CdTe nanoparticles in the hexagonal phase were obtained at high temperature (above 280°C), the cubic phase particles presented here are prepared at moderate temperatures (96°C). The mean cluster sizes obtained from the full width at half-maxima intensity of the (111) zinc blende reflection according to the Scherrer equation yields 1.9 nm. High-resolution electron microscopy studies revealed the existence of the lattice planes indicating high crystallinity of the samples. Additionally, a predominance of edged rhomboedric or tetrahedric crystallites is seen from the high-resolution electron microscopy micrographs. Thus, the shape of the clusters could not be considered to be near spherical but might be preferentially edged. This trend has also been observed in the literature in the case of the thiol-stabilized CdS clusters with comparable sizes.

Luminescence refers to the absorption of energy by matter, and its re-emission as visible or near-visible light. If A* denotes an excited state of a substance A, then luminescence consists of the emission of a photon,



where h is Planck's constant and ν is the frequency of the photon. A strong exciton luminescence peak at 2.3 eV dominates the emission spectrum of CdTe nanocrystals at room temperature. An exciton is a Coulomb correlated electron/hole pair in a semiconductor. The mean luminescence decay time of CdTe nanocrystals at room temperature decreases from 120 ns at 1.94 eV to 20 ns at 2.43 eV.¹⁸

3.2. Synthesis of Doped Nanowires from Doped Nanoparticles

One-dimensional crystalline CdTe nanowires will be synthesized by the spontaneous reorganization of CdTe nanoparticles synthesized by Weller's method. In this method, nanoparticles are found to spontaneously reorganize into crystalline nanowires upon controlled removal of the protective shell of organic stabilizer. The intermediate step in the nanowire formation is found to be pearl-necklace aggregates. Strong dipole-dipole interaction is believed to be the driving force of the nanoparticle self-organization. The linear aggregates subsequently recrystallized into nanowires whose diameter is determined by the diameter of the nanoparticles.

Removal of the stabilizer is essential for the formation of CdTe nanowires out of its nanoparticles. If the methanol precipitation and aqueous redissolution steps are excluded and the original excess thiol stabilizer remained in the solution, nanowires do not form. Therefore, the chain aggregation is initiated by the overall decrease of the stabilizer concentration, which results in the shift of the dynamic equilibrium between nanoparticle-bonded and free stabilizer toward its dissolved state. Furthermore, methanol is a better solvent for thioglycolic acid than water, which also contributes to the shift of the equilibrium.

For that reason, CdTe colloids will be precipitated by methanol addition and re-dissolved in pure water at pH 9.0. This results in the partial removal of the stabilizer. The resulting dispersion will be allowed to age in darkness at room temperature for several days. During this period the quantities of nanowires and their lengths will be

monitored by transmission electron microscopy (TEM) and tapping atomic force microscopy (AFM). Typically, the process of nanowire growth continues over a period of another 7 days.¹⁷

High-resolution transmission electron microscopy shows that CdTe nanowires produced in this manner are single-crystalline in structure, albeit with some defects.¹⁷ Lattice plane spacings calculated from the diffraction patterns are 3.98 Å hkl (100) and 2.29 Å hkl (110) and are typical for hexagonal wurtzite CdTe structures. The resulting nanowires are between several hundred nanometers and 10 microns long and they are uniform in diameter. Unlike many other nanowires from direct band-gap semiconductors with aspect ratios higher than 10 synthesized in the solution, CdTe nanowires that are produced have strong luminescence, which is a pertinent feature for many photonic devices, for instance sensors. Four different CdTe dispersions with luminescence maxima at 520 to 530 (green), 550 to 565 (yellow), 590 to 605 (orange), and 610 to 625 (red) nm were used as sources for the preparation of nanowires. The resulting nanowires are green nanowires, which are 2.5 nm, yellow nanowires 3.5 nm, orange nanowires 4.2 nm, and red nanowires 5.6 nm in diameter. The quantum yield of a luminescent substance is defined by;

$$\Phi_{\text{quantum yield}} = \frac{(\# \text{ of photons re-emitted})}{(\# \text{ of photons absorbed})} \quad (1)$$

The green nanowires had luminescence quantum yields as high as 29 %, while for yellow nanowires it was 16.2 %, for orange nanowires it was 6.0 %, for red nanowires it was 2.3 %.¹⁹ These numbers can be compared with the 5 to 10 % luminescence quantum yield of CdSe rods. The high luminescence quantum yields are indicative of the high degree of nanowire crystallinity. For all nanowire sizes, the luminescence was strong enough to observe the emission of single nanowires in a conventional confocal microscopy setup. The emission wavelength of the nanowire luminescence can be easily tuned by sizing the starting nanoparticles. The lengths of the luminescent rods in all images match very well with those seen in AFM and TEM. This means that the entire nanowire is optically active. The color of the nanowire emission remains the same over its entire length, which is reflective of the constancy of their diameter. The reasons that this method is chosen for one-dimensional nanowire synthesis are that it is straightforward and the quality of the produced nanowire is high. They display excellent uniformity in nanowire diameter, have a high aspect ratio, and a significant quantum yield. The selection of the original particle sizes offers convenient means for the control of the degree of quantum confinement and nanowire morphology.

4. Magnetic Alignment of Magnetic Ion Doped CdTe Nanowires

Inorganic solids with unpaired electrons have a magnetic moment, and the value of the magnetic moment of a body is a measure of the strength of the magnetism that is present. Atoms in various transition series of the periodic table have unfilled inner energy levels in which the spins of the electrons are unpaired, giving the atom a net magnetic moment. The magnetic properties of unpaired electrons arise from two causes, electron spin and electron orbital motion. Of most importance is the spin component. An electron may usefully be visualized as a bundle of negative charge spinning on its axis. The magnetic moment vector of a system with a total spin vector (S) is given by following equation,

$$\mu = (e/mc) S \quad (2)$$

where e is the charge of the electron, m is the mass of electron, c is the speed of light and S is the magnetic moment of the corresponding ion, for instance it is $5/2$ for Mn^{2+} , whereas it is $7/2$ for Eu^{2+} .

In a crystal each atom having a magnetic moment has a magnetic field about it. If the magnetic field is large enough, the resulting large DC magnetic field can force a nearest neighbor to align in the same direction provided the interaction energy is larger than the thermal vibrational energy of the atoms in the lattice.

In the case of a small particle such as an electron that has a magnetic moment, the application of a DC magnetic field forces its spin vector to align such that it can have only two projections in the direction of the DC magnetic field, which are $\pm 1/2 \mu_B$, where μ_B is the unit magnetic moment called the Bohr magneton.

The potential energy of a magnetic moment in an external magnetic field B is given by the following equation,

$$U = -\mu \cdot B \quad (3)$$

Therefore, when an ion that has a magnetic moment vector of μ is placed in an external magnetic field of B , μ will orientate itself such that it can have minimum potential energy. Since the dot product has a minimum value when the spin and the external field are parallel to each other, magnetic nanowires align parallel to the direction of external magnetic field.

Magnetic force is defined by the gradient of potential energy according to the following formula,

$$F_B = -\nabla U, F_B = \nabla (\mu \cdot B), \nabla = (\partial/\partial x)x + (\partial/\partial y)y + (\partial/\partial z)z \quad (4)$$

$$\nabla \text{ of dot product} = (\mu \cdot \nabla) \mathbf{B} + (\nabla \cdot \mu) \mathbf{B} + (\nabla \cdot \mathbf{B}) \mu + (\mathbf{B} \cdot \nabla) \mu \quad (5)$$

Among four components, first two components cancel due to \mathbf{B} is uniform and the third term cancels due to μ is linear, which is why its curl is zero. Therefore,

$$\mathbf{F}_B = (\mathbf{B} \cdot \nabla) \mu = B_x (\partial / \partial x) (\mu) + B_y (\partial / \partial y) (\mu) + B_z (\partial / \partial z) (\mu) \quad (6)$$

Since the magnetic field is on the z direction, only z component is taken into consideration and the direction of \mathbf{F}_B depends on the direction of μ , where direction of μ depends on the orientation of the nanowire in the solution. Therefore, \mathbf{F}_B does not have a certain direction, it applies torque on the nanowire in such directions that the nanowire can be aligned in the direction of the magnetic field to minimize its potential energy.

In one of the few related studies found in the literature, Nickel nanowires prepared by electrochemical growth in alumina templates have been removed from their templates and functionalized with luminescent porphyrins.²³ The response of the nanowires towards magnetic fields was quantified using video microscopy. In viscous solvents, magnetic fields could be used to orient Ni nanowires; however in mobile solvents Ni nanowires formed chains in a head-to-tail configuration when a small magnetic field is applied. Even in the most viscous solvents, the nanowires responded to the torques produced by small uniform magnetic fields, and aligned parallel to the field. Magnetic field gradients, produced either by external magnets or by neighboring nanowires, exert forces on the nanowires, and provide means to manipulate and assemble them. For example, the 1000 G/cm field gradient produced by a small bar magnet, placed outside an experimental cell containing approximately 3 cm³ of a water suspension, allows rapid collection of all the nanowires at the side of the cell in times of order 30 s. For nanoparticles in fluid suspension, the Reynolds number R is very small, and hence viscous drag dominates all other hydrodynamic effects. Thus, in response to an applied force F , a nanoparticle obtains a velocity of

$$\mathbf{v} = F/D \quad (7)$$

where D is the appropriate drag coefficient. This relationship holds for particles moving under gravitational settling, electric (electrophoresis), or magnetic forces.

A high magnetic field is an efficient and direct means to align carbon nanotubes also. Fujiwara et al. found that a high magnetic field of 7 T aligns arc-grown MWNTs.²⁴

They dried MWNT dispersion in methanol under a constant magnetic field and observed the MWNTs alignment parallel to the field. This result was explained by the difference between the diamagnetic susceptibilities parallel and perpendicular to the tube axis; if perpendicular one is larger than the parallel one; a MWNT tends to align parallel to the magnetic field by overcoming thermal energy. It is shown that the MWNTs are aligned in a polyester matrix through polymerizing a MWNT-monomer dispersion inside a magnet. The monomer solution of unsaturated polyester is mixed with MWNTs and subjected to a constant magnetic field of 10 T. Polymerizing this MWNT-monomer dispersion under the magnetic field freezes the alignment of MWNTs in the polymer matrix. For the MWNT alignment, the magnetic anisotropy of a MWNT must be high enough to overcome thermal energy of Brownian motion and resistance against rotating in the viscous monomer solution.

Semiconductors do not have any reported magnetic dipoles, basically because of restricted motion of their electrons, which is also the case for both CdTe nanoparticles and nanowires. However, it is expected that doping magnetic ions into the crystal lattices of CdTe nanoparticles will provide enough magnetism for alignment of magnetic ion doped CdTe nanowires.

Experimentally, doped CdTe nanowire solutions will be placed in a magnetic field with a magnitude of 5 Tesla or higher. Depending upon the results, varying magnitudes of magnetic fields will be tried. Substrates such as Silicon substrates will be dipped into the solution of nanowires in the direction of magnetic field and they will be pulled out slowly afterwards. The wires are expected to align in the direction of the magnetic field on the substrates by the help of both magnetic field and gravitational settling.

A second method, with a little difference from the first method, will also be tried to obtain aligned nanowires in a more organized and permanent fashion. For that reason, Silicon substrates will first be dipped into the solutions of different positively charged polyelectrolyte macromolecular adsorption promoters, such as PDDA (diallyldimethyl- ammonium chloride) or PEI (polyethylenimine). Polyelectrolytes are expected to deposit on the surface of the silicon substrates due to the electrostatic and short range van der Waals interactions.²⁶ Silicon substrates deposited with polyelectrolytes will be dipped into the solution of magnetic ion doped CdTe nanowires, those are already aligned under the very strong magnetic field. Therefore, it is expected that nanowires can deposit onto the silicon substrates in a more organized and permanent fashion due to the electrostatic interaction between the polyelectrolytes and the nanowires. In both of the methods, after the substrates dipped into the solution of nanowires

under magnetic field, they will be left to dry for imaging of the substrate surface with tapping mode AFM.

5. Characterization Techniques

5.1. XRD (X-ray Diffraction)

In the proposed research, powder X-ray diffraction method will be performed using a powdered both doped and undoped CdTe nanoparticle samples. According to the positions of the reflection peaks, the crystalline structure of doped CdTe nanocrystals will be assigned, which is expected to be the same crystalline structure of undoped CdTe nanocrystals, that is, predominantly cubic blende phase crystalline structure.¹⁶ For all dopant concentrations, additional peaks or impurity phases in the XRD pattern, that are possible due to any impurities will be sought and observation of the peak broadening in XRD pattern of the samples will indicate that nanoparticles are really present in the sample.

Furthermore, the average particle sizes can be calculated from the width of XRD broadening by using Scherrer's equation,

$$t = 0.9\lambda / \beta \cos\theta \quad (8)$$

where t is the particle diameter in Å, λ is the wavelength of X-rays, β is the half-width of the diffraction peak at 2θ , and θ is the diffraction angle. A random ion displacement is foreseen to describe the dopant substitution into the cationic Cd site in cubic blende lattice symmetry, which allows the use of Vegard's law, an approximate empirical law which holds that a linear relation exists, at constant temperature, between the crystal lattice constant of an alloy and the concentrations of the constituent elements.²¹ Statistical substitution of dopants into a lattice site is predicted to lead to a lattice contraction for smaller ions and a lattice expansion for larger ions. Isolation of the defect ions at surface sites or at interstitial sites will result in insignificant lattice shifts arising primarily from strain effects. Therefore, shifts in the a-lattice parameters will be observed against dopant concentrations. The observation of a linear shift with increasing dopant concentrations will be in accord with the predictions of Vegard's law, suggesting displacement occurs at the lattice sites situated both in the core and on the surface through a purely statistical process, and not isolation of the defect ion only at the surface and interstitial sites through an ion-migration pathway.¹¹

5.2. SQUID (Superconducting Quantum Interference Device)

When crystals such as bulk iron are formed from atoms having a net magnetic moment, a number of different situations can occur relating to how the magnetic moments of the individual atoms are aligned with respect to each other. If the

magnetic moments are randomly arranged with respect to each other, then the crystal has a zero net magnetic moment, and this is referred to as the paramagnetic state. The application of a DC magnetic field aligns some of the moments, giving the crystal a small net moment. In a ferromagnetic crystal these moments all point in the same direction even when no DC magnetic field is applied, so the whole crystal has a magnetic moment and behaves like a bar magnet producing a magnetic field outside of it. If a crystal is made of two types of atoms, each having a magnetic moment of a different strength, it is called ferrimagnetic. Such a crystal will also have a net magnetic moment, and behave like a bar magnet. In an antiferromagnet the moments are arranged in an antiparallel scheme, that is, opposite to each other, and hence the material has no net magnetic moment.

The interaction between atomic magnetic moments is of two types: the so-called exchange interaction and the dipolar interaction. The exchange interaction is a purely quantum-mechanical effect, and is generally the stronger of the two interactions. It represents the difference in the Coulomb energy between two electrons with spins that are parallel and antiparallel. Under certain assumptions the exchange interaction can be written in a simple form as the following equation,

$$V_{ij} = J \cdot S_i \cdot S_j \quad (9)$$

where J is the coupling strength, which is determined by the distance between neighboring moments and the background medium. This is the form used in the Heisenberg model of magnetism. For a ferromagnet, J is negative, while for an antiferromagnet it is positive. The exchange interaction, because it involves overlap of orbitals, is primarily a nearest-neighbor interaction.

Temperature-dependent magnetization measurements of both magnetic ion doped CdTe nanocrystals and nanowires will be conducted using SQUID. Thin films of nanocrystals and nanowires will be deposited onto a glass substrate and then scraped into the sample holder for the measurements. The sample holder diamagnetism will be subtracted from the raw magnetization data. Pure CdTe nanocrystals and nanowires will be measured as baselines and they will be expected to be diamagnetic.¹⁰ The magnetic susceptibility χ (T) will be measured in the temperature range from 5 to 300 K at 0.1 T according to the formula:

$$\chi = M/H \quad (10)$$

where M is the magnetization at low field and H is the external field.³ The field dependence of magnetization M will be measured up to 5 T at 5 K. The magnetic hysteresis loop will be plotted and coercivity and remanence temperature dependence

will be collected. Rapid magnetization at low fields and a clear magnetic hysteresis will be indicative of magnetism and therefore Curie-Weiss behavior will be expected, where χ (T) is defined by the following formula,

$$\chi(T) = C/(T-\theta) + \chi_0 \quad (11)$$

where C, θ , and χ_0 are the Curie constant, Curie-Weiss temperature, and the temperature independent susceptibility, respectively. The Curie constant is described as $C = Ng^2S(S+1)\mu_B^2/3k_B$, where N is the number of magnetic ions, $g=2$, $S=5/2$ for Mn^{2+} for instance, μ_B the Bohr magneton, and k_B the Boltzman constant. Experimental C values will be determined and using the theoretical C value (4.38 emu K/mol for Mn^{2+} for instance), the actual doping concentration of Mn^{2+} ions will be estimated. This percentage estimation will also correspond to a certain number of Mn^{2+} ions per nanocrystal, which will help to understand the mechanism of magnetism. Furthermore, comparison of the experimental and theoretical C values will make it possible to determine whether Eu^{2+} and Eu^{3+} coexist in the nanocrystal structure or not.⁶

5.3. AFM (Atomic Force Microscopy)

In the proposed research, AFM will be the main device to monitor the degree of alignment of magnetic ion doped CdTe nanowires. AFM will also be used to monitor the shapes of the magnetic ion doped CdTe nanocrystals and CdTe nanowires.¹⁷

5.4. HRTEM (High Resolution Transmission Electron Microscopy)

In the proposed research, TEM will be used complementarily to XRD and AFM both to verify the crystal structure and to image magnetic ion doped CdTe nanoparticles and nanowires. The existence of lattice planes will confirm the crystallinity of samples and lattice plane spacings can be matched with the literature values, which will confirm the crystalline structure. The average particle sizes and shapes will be estimated as well.^{9,22}

5.5. ICP (Inductively Coupled Plasma)

In the proposed research, ICP will be the main method to determine the actual concentrations of dopant ions in CdTe nanocrystals as well as in CdTe nanowires. ICP measurements will be performed at particular wavelengths for each ion, for instance at 382 nm for Eu atom, and 214.4 nm for Cd atom.¹¹ The samples for analyses will be prepared by digestion of known amount of nanoparticles in nitric acid followed by dilution with water.

5.6. EPR (Electron Paramagnetic Resonance)

In the proposed research, EPR will be used to determine the dopant sites, such as a substitutional site or a non-substitutional anisotropic site.¹⁰ Further, EPR will be used to explain the bonding characteristics between dopant atoms and host lattices since hyperfine splitting constants depend on the environments of dopant atoms. For instance, a well-resolved hyperfine splitting is characteristic for isolated dopant ions, which suggests that dopant-dopant interactions are rather weak establishing that the dopant ions are randomly distributed in the host lattice without any significant clustering.⁸

5.7. XPS (X-Ray Photoelectron Spectroscopy)

In the proposed research, XPS will be used to determine both the composition of the doped samples as a complementary method to the ICP and the oxidation states of the dopants. For instance, the energy of transitions for $3d_{5/2}$ and $3d_{3/2}$ of Eu will allow assignment of the Eu valence by comparison to a bulk sample of Eu_2O_3 . In addition, a shift in Cd_{MNN} and Te 4p lines to lower or higher energies will mean that the Cd(II) and Te sites are perturbed by the presence of the dopant ions in the lattice.¹¹

XPS is mainly a surface technique and it is more likely that surface atoms will be in their higher oxidation states in contrast to the inner core atoms. Also, composition of the sample determined by XPS may be the composition at the surface, which might be similar or substantially different than the actual composition of the sample depending on whether the dopants are incorporated into the crystalline structure or not. However, XPS depth is predicted to be ~ 5 nm within the nanocrystalline structure and doped CdTe nanocrystals and nanowires are expected to have diameters less than 5 nm. Therefore, it is expected that XPS results could be used to determine the compositions of samples and the oxidation states of the dopants accurately.

References

1. Pena, D. J.; Razavi, B.; Smith, P. A.; Mbindyo, J. K.; Natan, M. J.; Mayer, T. S.; Mallouk, T. A.; Keating, C. D.; Electrochemical synthesis of multi-material nanowires as building blocks for functional nanostructures, *Mat. Res. Soc. Symp.*, **2001**, 636, D4.6.1-5
2. Fasol, G., Selective Electrodeposition of magnetic and metallic nanowires: A new approach to a fundamental technology, *Eurotechnology Japan K. K.*, **1998**
3. Feltn, N.; Levy, L.; Inger, D., Unusual static and dynamic magnetic properties of $Cd_{1-x}Mn_xS$ nanocrystals, *J. of Applied Physics*, **2000**, 87, 3, 1415-1423

4. Stowell, C. A.; Wiacek, R. J.; Saunders, A. E.; Korgel, B. A.; Synthesis and characterization of dilute magnetic semiconductor manganese-doped indium arsenide nanocrystals, *Nanoletters*, **2003**, 3, 10, 1441-1447
5. Jun, Y.; Jung, Y.; Cheon, J., Architectireal control of magnetic semiconductor nanocrystals, *J. of Am. Chem. Soc.*, **2002**, 124, 4, 615-619
6. Tsujii, N.; Kitazawa, H.; Kido, G., Magnetic properties of Mn and Eu doped ZnS nanocrystals, *J. of Applied Physics*, **2003**, 93, 10, 6957-6959
7. Schrier, J.; Whaley, K. B., A simple model for magnetization ratios in doped nanocrystals, *Condensed Matter*, **2003**, 1-8
8. Viswanatha, R.; Sapra, S.; Gupta, S. S.; Satpati, B.; Satyam, P. V.; Dev, B. N.; Sarma, D. D., Synthesis and characterization of Mn-doped ZnO nanocrystals, *J. Phys. Chem. B*, **2004**, 108, 6303-6310
9. Schwartz, D. A.; Norberg, N. S.; Nguyen, Q. P.; Parker, J. M.; Gamelin, D. R.; Magnetic quantum dots: Synthesis, spectroscopy, and magnetism of Co^{2+} and Ni^{2+} doped ZnO nanocrystals, *J. of Am. Chem. Soc.*, **2003**, 125, 13205-13218
10. Stowell, C. A.; Wiacek, R. J.; Saunders, A. E.; Korgel, B. A., Synthesis and characterization of dilute magnetic semiconductor manganese-doped indium arsenide nanocrystals, *Nanoletters*, **2003**, 3, 10, 1441-1447
11. Raola, O. E.; Strouse, G. F., Synthesis and characterization of Eu-doped cadmium selenide nanocrystals, *Nanoletters*, **2002**, 2-12, 1443-1447
12. Bol, A. A.; Beek, R.; Meijerink, A., On the incorporation of trivalent rare earth ions in II-VI semiconductor nanocrystals, *Chem. Mater.*, **2002**, 14, 1121-1126
13. Inger, D.; Pileni, M. P., Limitations in producing nanocrystals using reverse micelles as nanoreactors, *Advanced Functional Materials*, **2001**, 11, 2, 136-139
14. Inger, D.; Feltn, N.; Levy, L.; Gouzerh, P.; Pileni, M. P., CdTe quantum dots obtained by using colloidal self-assemblies as templates, *Advanced Materials*, **1999**, 11-3, 220-223
15. Pileni, M. P., The role of soft colloidal templates in controlling the size and shape of inorganic nanocrystals, *Nature Materials*, **2003**, 2, 145-150
16. Rogach, A. L.; Katsikas, L.; Kornowski, A.; Su, D.; Eychmuller, A.; Weller, H., Synthesis and characterization of thiol-stabilized CdTe nanocrystals, *Ber. Bunsenges. Phys. Chem.*, **1996**, 100, 1772-1778
17. Tang, Z.; Kotov, N. A.; Giersig, M., Spontaneous organization of single CdTe nanoparticles into luminescent nanowires, *J. of Science*, **2002**, 297, 237-240
18. Kapitonov, M.; Stupak, A. P.; Gaponenko, S. V.; Petrov, E. P.; Rogach, A. L. Eychmuller, A., Luminescence properties of thiol stabilized CdTe nanocrystals, *J. Phys. Chem B*, **1999**, 103, 10109-10113
19. Kalaugher, L., CdTe nanowires make themselves up, *nanotechweb.org*, july **2002**
20. Deka, S.; Pasricha, R.; Joy, P. A., Synthesis and ferromagnetic properties of lightly doped nanocrystalline $\text{Zn}_{1-x}\text{Co}_x\text{O}$, *Chem. Mater.*, **2004**, 16, 1168-1169
21. Denton, A. R.; Ashcroft, N. W., Vegard's Law, *Physical Review A*, **1991**, 43, 6, 3161-3164
22. Song, W. L.; Lee, B. I.; Wang, Z. L.; Tong, W.; Wagner, B. K.; Park, W.; Summers, C. J., Synthesis and photoluminescence enhancement of Mn^{2+} -doped ZnS nanocrystals, *Journal of Luminescence*, **2001**, 92, 73-78
23. Tanase, M.; Bauer, L. A.; Hultgren, A.; Silevitch, D. M.; Sun, L.; Reich, D. H.; Searson, P. C.; Meyer, G. J., Magnetic alignment of fluorescent nanowires, *Nanoletters*, **2001**, 1, 3, 155-158
24. Kimura, T.; Ago, H.; Tobita, M.; Ohshima, S.; Kyotani, M.; Yumura, M., Polymer composites of carbon nanotubes aligned by a magnetic field, *Advanced materials*, **2002**, 14, 19, 1380-1383
25. Tang, Z.; Wang, Y.; Kotov, N. A., Semiconductor nanoparticles on solid substrates: film structure, intermolecular interactions, and polyelectrolyte effects, *Langmuir*, **2002**, 18, 7035-7040
26. Yang, P.; Lu, M.; Xu, D.; Yuan, D.; Song, C.; Liu, S.; Cheng, X., Luminescence characteristics of ZnS nanoparticles codoped with Ni^{2+} and Mn^{2+} , *Optical Materials*, **2003**, 24, 497-502